ON THE IMPLEMENTATION OF THE EQUIVALENCE THEOREM IN THE HYBRID FDTD-MoMTD TECHNIQUE

M. A. Hernández-López (*), A. Rubio Bretones (**), M. Quintillán (*) and R. Gómez Martín (**)

(*) Dep. Física Aplicada, Salamanca (Spain)

(**) Dep. Electromagnetismo y Física de la Materia, Facultad de Ciencias, 18071, Granada (Spain),

email: rgomez@goliat.ugr.es

ABSTRACT. *The hybrid FDTD-MoMTD technique is a powerful tool for analysing the transient excitation of inhomogeneous permeable bodies by arbitrary thin-wire antennas. This technique is based upon the calculation of the equivalent electric and magnetic currents on a Huygen's surface that encloses the antenna. This paper studies, by means of several numerical experiments, the effects on the accuracy of the results of the size of the Huygen's box, the size of the spatial increment in the FDTD algorithm and the distance from the Huygen's surface to the observation point.*

1 INTRODUCTION

A hybrid technique that efficiently combines two powerful numerical methods, the Finite Difference Time Domain (FDTD) and the Method of Moments in the Time Domain (MoMTD), was recently described in [1]. This technique, which is applicable to complex geometries comprising thin-wire structures and arbitrary inhomogeneous dielectric bodies, has been successfully used to study linearly and non-linearly loaded broadband antennas near arbitrary inhomogeneous bodies and to simulate a three dimensional Ground Penetrating Radar (GPR) [2]-[3].

The hybridization is based upon the surface equivalence theorem (Huygen's principle) [4] and it is implemented, using a time-stepping procedure, as follows [1]:

1) An imaginary closed Huygens's surface S_H is located around the thin-wire antenna. At each time step, the equivalent sources on S_H are derived from the fields radiated by the antenna in free space by applying the MoMTD.

2) Next, the FDTD algorithm is applied to compute the fields in the entire computational domain, removing the antenna inside S_H and replacing it by the equivalent sources. Thus, according to the equivalence principle, we obtain the total field outside S_H and just the field scattered by the inhomogeneous part of the configuration inside S_H.

3) The FDTD solution inside S_H when the antenna is not present is the extra incident field on this antenna needed to compute, by the MoMTD, the currents induced on its surface and subsequently the radiated fields and the equivalent sources on S_H.

This paper studies the effect of the size of the FDTD cell used to model S_H and the size of S_H itself on the precision of the method. To this end, a Hertzian (infinitesimal) dipole, placed at the center of S_H, was chosen as a radiation source. This choice allowed us to use the known closed-form solution for the fields created by the Hertzian dipole to calculate their exact values at the points of interest and to make S_H arbitrarily small around the radiation source. The difference between the values of the fields derived using their analytical expressions and the ones obtained using the hybrid method are calculated as a function of the size of the FDTD cell on S_H and of the size of S_H itself. The next section describes the numerical experiments that have been carried out and the results obtained.

2 NUMERICAL EXPERIMENTS AND RESULTS

The basic geometry used for the numerical experiments is shown in Figure 1, where the arrow represents a Hertzian dipole oriented along the z axis, positioned at the center of the Huygen's surface S_H and radiating in free space. The external surface S_B is where the FDTD algorithm is truncated by applying suitable absorbing boundary conditions. The FDTD cells, as well as S_H and S_B, are assumed to be cubic and the volume V_H inside S_H is uniformly discretized using a cell size Δ. If the Hertzian dipole radiates in free space, according to the equivalence theorem, there will be no scattered field inside S_H and the total field should be zero. We chose three observation points: P_1 and P_2 outside S_H and P_3 at the center of the Huygen's volume. P_1 is located at a fixed position, (0.48,-0.1,-0.36) m, while the coordinate of the observation point P_2 depends on the size of S_H in such a way that it always remains at a distance of two FDTD cells from S_H. The fields at all these points are calculated

1054-4887 © 2000 ACES

both numerically, using the hybrid method, and analytically from the expressions [5].

$$\mathbf{E}(\mathbf{r},t) = \frac{1}{4\pi\varepsilon}\left\{\left(\frac{1}{r^3}\int[i]dt + \frac{[i]}{cr^2}\right)\left(3(\hat{z}.\hat{r})\hat{r} - \hat{z}\right) + \frac{1}{c^2 r}\frac{d[i]}{dt}\left(\hat{r}\times(\hat{r}\times\hat{z})\right)\right\}$$
$$\mathbf{H}(\mathbf{r},t) = \frac{1}{4\pi}\left(\frac{1}{cr}\frac{d[i]}{dt} + \frac{[i]}{r^2}\right)(\hat{z}\times\hat{r}) \qquad (1)$$

where $i=i(t)$ is the transient current excitation, r is the radial distance from the center of the Hertzian dipole to the observation point, $\hat{r}$ and $\hat{z}$ are unit vectors, and the rectangular brackets denote that the variables contained within them are to be evaluated at the retarded time $t'=t-r/c$. The expressions in (1) are also used to calculate the equivalent electric and magnetic currents from the tangential component of the fields on the surface S_H.

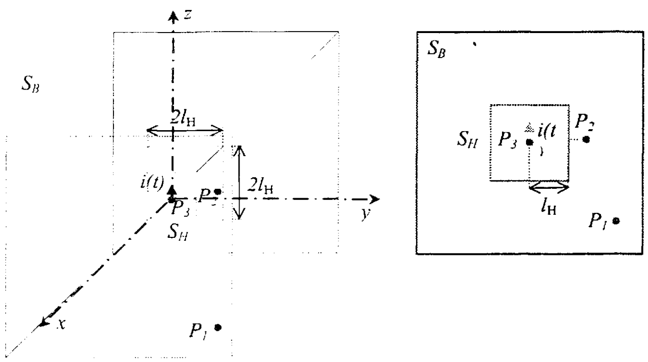

a) b)

Figure 1.- a) Geometry for the Hertzian dipole radiating in free space; b) Projection on the plane x=0.

Henceforth the transient current excitation will be particularized for a differentiated Gaussian pulse current defined as

$$i(t) = -2g^2(t-t_{max})\exp\left[-g^2(t-t_{max})^2\right] \qquad (2)$$

where $g=10^9$ s^{-1} and $t_{max}=4/g$.

At the points P_1 and P_2 (outside S_H) an error factor, Q_1, is defined as the sum of the normalized root-mean square error of each component of the electric field, that is:

$$Q_1 = \sum_{\alpha=x,y,z} Q_{1,\alpha}; \qquad Q_{1,\alpha} = \sqrt{\frac{\sum_{n=0}^{N}\left|E_\alpha^T(n) - E_\alpha^N(n)\right|^2}{\sum_{n=0}^{N}\left|E_\alpha^T(n)\right|^2}} \qquad (3)$$

where N is the total number of time intervals and $E_\alpha^T(n)$ and $E_\alpha^N(n)$ represent the values, at time step n, of the α electric field component calculated using expression (1) and the hybrid method respectively.

At point P_3 (inside S_H), as previously stated, the total field should be null unless a scattered field exists. To calculate an error factor similar to Q_1 inside S_H, a known scattered electromagnetic field is required there. To this end, a perfect electric conducting (PEC) plate is introduced into the original geometry at a fixed distance, d_C=0.2 m, from the center of the Huygens's zone as shown in Figures 2a-c. The expression of the field inside S_H, scattered by the PEC, can be also obtained from (1) by replacing the PEC surface by the image of the original radiation source (see Figure 3). Then, an error factor, Q_2, inside S_H is defined as

$$Q_2 = \sum_{\alpha=x,y,z} Q_{2,\alpha}; \qquad Q_{2,\alpha} = \sqrt{\frac{\sum_{n=0}^{N}\left|E_\alpha^{Ti}(n) - E_\alpha^N(n)\right|^2}{\sum_{n=0}^{N}\left|E_\alpha^{Ti}(n)\right|^2}} \qquad (4)$$

where $E_\alpha^{Ti}(n)$ and $E_\alpha^N(n)$ represent the values of the electric field components at P_3 calculated using the image of the radiation source and the hybrid method respectively. To calculate Q_2, the effect of the undesired return from S_H due to the staggered position of the equivalent electric and magnetic currents [5] has been eliminated. This was carried out by time gating when there is no overlapping between the undesired and the desired signals or, if overlapping exists, calculating the field inside S_H with the Hertzian dipole radiating in the free space and subtracting these results from those obtained including the PEC.

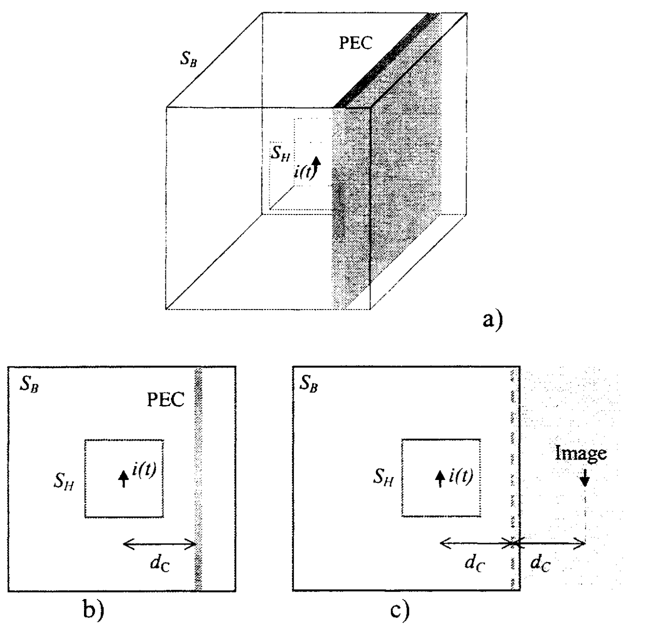

Figure 2.- a) Hertzian dipole in front a PEC interface; b) Projection on the x=0 plane; c) Equivalent problem including the image source.

To study the effects of the size of the FDTD cell and S_H, the error factors Q_1 and Q_2 have been evaluated for three different cases:

i) Keeping the value of Δ constant and changing the size of S_H (Figure 3).

ii) Changing the value of Δ and maintaining the number of cells inside S_H constant which, in consequence, does not remain constant (Figure 4).

iii) Changing the value of Δ while the size of S_H is unchanged (Figure5).

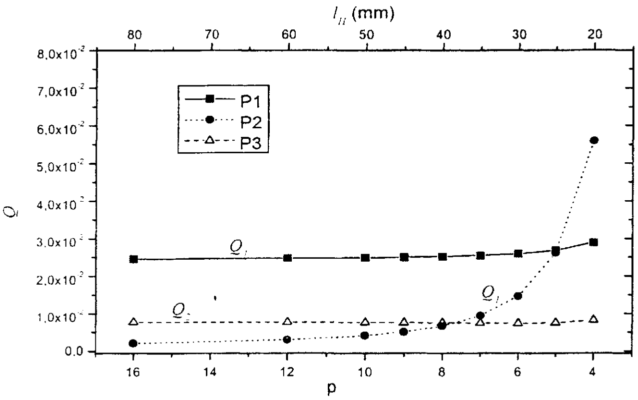

Figure 3.- Error factors at the observation points as a function of l_H and the number of cells inside S_H for a fixed value of $\Delta = 5$ mm.

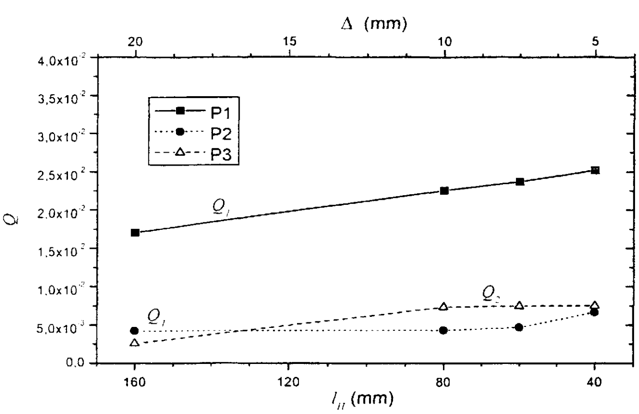

Figure 4.- Error factors at the observation points as a function of l_H and the cell size Δ keeping p=8.

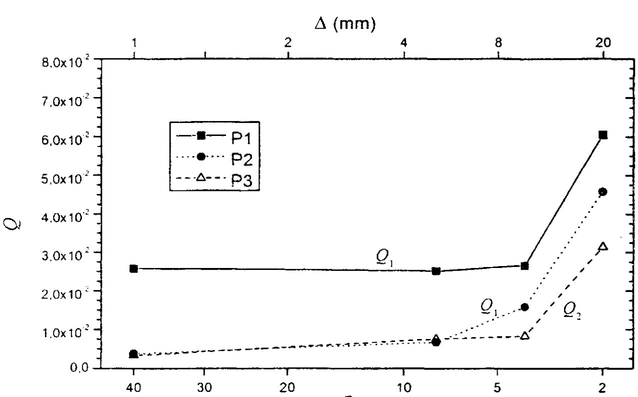

Figure 5.- Error factors at the observation points as a function of the cell size Δ and the number of cells inside S_H for a fixed size of S_H.

The parameter p in Figures 3 and 5 is an integer number, such that, the half length l_H of one side of S_H, is given by $l_H=p\,\Delta$ and the surface of S_H equals $24(p\,\Delta)^2$ (see Figure 2). Moreover, in all cases, the principal spectral components have been resolved with at least 15 cells per wavelength.

Figure 3 shows how the error factors Q_1 and Q_2 increase as l_H decreases while the value of $\Delta = 5$ mm is kept constant. This can be explained from the dependence upon r as $1/r^2$ and $1/r^3$ of the near-field contributions to the total field in (1). When l_H decreases the influence of the near fields increases and a smaller value of Δ would be necessary to get a greater number of points on l_H in order to take into account the strong dependence of the near fields upon r. On the contrary, when l_H increases, the smoother variation of the amplitude of the fields allows us to use a greater value of Δ. Another way of illustrating this effect is given in Figure 4, which shows that Q_1 and Q_2 increase when l_H decreases even though Δ also decreases. The method used to decrease l_H was to keep the parameter p constant (p=8) in $l_H=p\,\Delta$ while Δ decreases.

For a fixed value of l_H =40 mm, the dependence upon Δ of the error factors Q_1 and Q_2 is shown in Figure 5. As expected, in the three cases the error factors decrease as Δ decreases because the number of field samples on l_H increases.

Figures 6a-b show the temporal evolution of the three electric field components calculated numerically and analytically in the cases where greater values of the error factors, represented in Figures 3 and 4, were found. These correspond to point P_2 for l_H =20 in Figure 4 and point P_1 for l_H =40 in Figure 5. It can be observed that even in these cases the agreement between the numerical and analytical results is very good. All these results show that the method works properly even when the Huygen's surface is small and the observation point is near the surface. With regard to this, the smallest S_H that we were able to implement (in a 600 MHz PC with 768 Mbytes of RAM) had l_H =10 mm and was modeled with Δ =1 mm (l_H =10 Δ) with P_2 being at 2 mm from S_H or equivalently at 1.2 cm from the radiation source. In this case, not included in the previous plots, the value obtained for Q_1, at point P_2, was Q_1=0.0673. Figure 7 shows the three electric field components calculated numerically and analytically at this point. Again, it is observed that there is very good agreement. It should be pointed out that similar conclusions to the ones includes in this paper were obtained for narrower gaussian excitations.

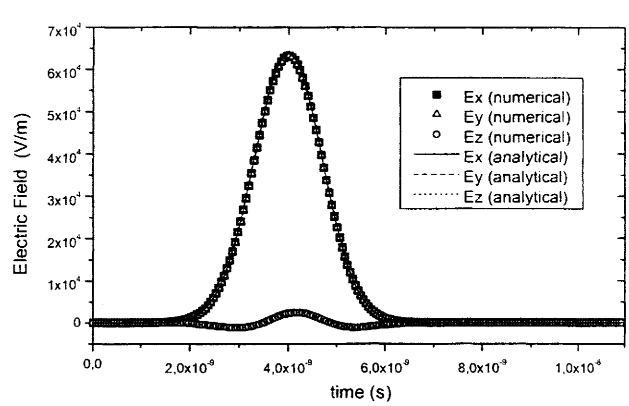

a)

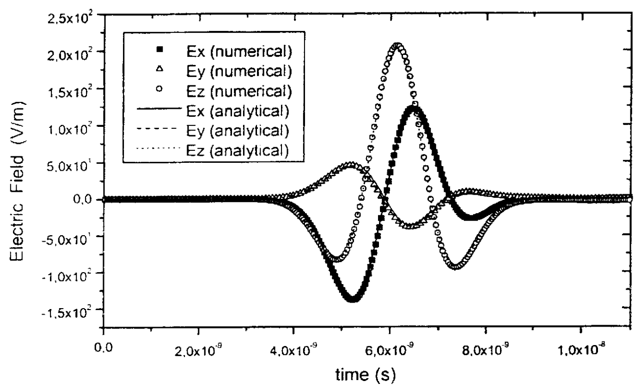

b)

Figure 6.- Temporally evolution of the electric field calculated numerically and analytically. a) Point P_2 for l_H =20; b) Point P_1 for l_H =40.

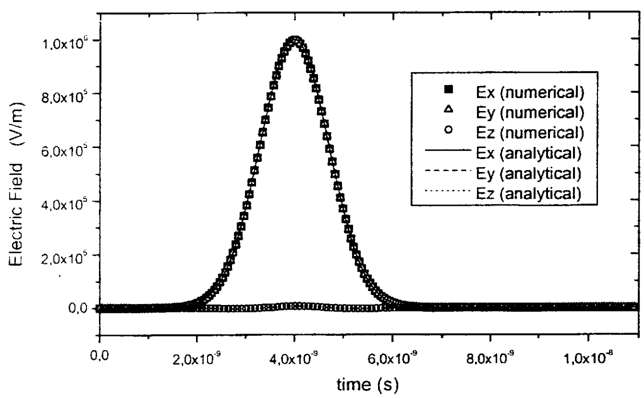

Figure 7.- Temporally evolution of the electric field calculated numerically and analytically to point P_2 for l_H =10 mm.

3 CONCLUSIONS

This paper studies the effects of the following parameters on the accuracy of the results obtained by the hybrid FDTD-MoMTD technique: the size of the Huygen's box around the antenna, the size of the spatial increment in the FDTD algorithm and the distance from the Huygen's surface to the observation point. By means of several numerical experiments the method is shown to be robust and gives very good results even when the Huygens's'surface is very near the radiation source.

Acknowledgement

This paper has been partially supported through the projects TIC99-0624 and TIC98-1037-C03-01.

4 REFERENCES

[1] A. Rubio Bretones, R. Mittra and R. Gómez Martín, "A new Hybrid Method Combining the Method of Moments in the Time Domain and FDTD", *IEEE Microwave and Guided Wave Letters,* vol.8, pp. 281-283, 1998.

[2] A. Rubio Bretones and R. Gómez Martín, "Study of Thin-Wire Broadband Antennas Near an Inhomogeneous Medium Using a Time-Domain Hybrid Technique" *International Conference on Electromagnetics in Advanced Applications (ICEAA 99)*, pp. 681-682, Torino (Italy), September 1999.

[3] A. Rubio Bretones, S. González García and R. Gómez Martín, " Análisis of Thin-Wire Broadband Antennas near an Inhomogeneous Medium. Simulation of a Ground Penetrating Radar", *ISRANT' 99 Proceedings*, pp704-706, Málaga (Spain), December 1999.

[4] C. A. Balanis "Advanced Engineering Electromagnetics" *John Wiley*, 1989.

[5] R. Gómez Martín, J. A. Morente, B. G. García "Some Thoughts About the radiation of Antennas Excited by Non-Sinusoidal Currents" *Int. Journal Elctronics*, vol.57, no. 5, pp 617-625; 1984.

[6] J. G. Maloney and G. S. Smith "Modeling of Antennas" in "Advances in Computational Electrodinamics: The Finite-Difference Time-Domain Method " A. Taflove, Editor; *Artech House* 1998.